ResearchGate

See discussions, stats, and author profiles for this publication at: https://www.researchgate.net/publication/305452638

# Automatic Generation Control of Thermal Power System under Varying Steam Turbine Dynamic Model Parameters Based on Generation Schedules of the Plants

**Article** *in* The Journal of Engineering · July 2016

DOI: 10.1049/joe.2016.0178

CITATIONS
10

READS
1,830

**3 authors:**

Nikhil Pathak
Tsinghua University
**23** PUBLICATIONS **76** CITATIONS

SEE PROFILE

T. S. Bhatti
Indian Institute of Technology Delhi
**155** PUBLICATIONS **2,632** CITATIONS

SEE PROFILE

Ashu Verma
Indian Institute of Technology Delhi
**85** PUBLICATIONS **660** CITATIONS

SEE PROFILE

**Some of the authors of this publication are also working on these related projects:**

Computationally Efficient Linear Optimal Power Flow for Power System Applications View project

Energy Management and Resource Optimization of Smart Cyber-Physical Distribution System with Demand Response And Electric Vehicles View project

All content following this page was uploaded by Nikhil Pathak on 09 April 2019.

The user has requested enhancement of the downloaded file.

# Automatic generation control of thermal power system under varying steam turbine dynamic model parameters based on generation schedules of the plants

*Nikhil Pathak, Ashu Verma, Terlochan Singh Bhatti*

*Centre for Energy Studies, Indian Institute of Technology Delhi, New Delhi 110016, India*
*E-mail: 2013niks@gmail.com 24 6 2016*

Published in *The Journal of Engineering*; Received on 13th June 2016; Revised on 24th June 2016; Accepted on 29th June 2016

**Abstract:** This paper investigates the automatic generation control (AGC) of thermal power system operating under different power generation levels/schedules of the plants. The power system load varies considerably over the period of 24 hours and accordingly thermal power plants are planned to operate at different generation schedules. It has been discovered that the steam turbine dynamic model parameters also changes along with generation schedules of the plant. Typical steam turbine model parameters are the turbine time constants and power fractions. The literature survey reveals that steam turbine dynamic model parameters are assumed to be constant in all preceding studies pertaining to AGC systems, irrespective of generation schedules of the plant. In this paper, steam turbine dynamic model parameters have been computed for an actual 500 MW thermal unit at different generation schedules. These steam turbine dynamic model parameters have been used to study the dynamic performance of AGC system. The paper also presents the general mathematical procedure to calculate steam turbine dynamic model parameters from an actual generating unit using the heat balance data of a thermal power plant. Results for two area thermal power system demonstrate the potential of the proposed approach.

**Nomenclature**

*List of symbols*

| | |
|---|---|
| $i$ and $j$ | index number referring to the $i$th and the $j$th areas (where $i$ and $j = 1, 2, \ldots$) |
| $\Delta f_i$ | deviation in frequency of the $i$th area (Hz) |
| $\Delta P_{\text{tie}ij}$ | deviation in tie-line power (pu) |
| $D_i$ | load damping constant of the $i$th area (MW pu/Hz) |
| $K_{\text{p}i}$ | $1/D$ power system rotating mass gain of the $i$th area (Hz/MW pu) |
| $T_{\text{p}i}$ | power system time constant in the $i$th area (s) |
| $\text{ACE}_i$ | area control error signal in the $i$th area |
| $P_{\text{r}i}$ | rated capacity of the $i$th area (in MW) |
| $R^i_{\text{eqv}}$ | equivalent speed droop characteristic of generating unit in the $i$th area (Hz/MW pu) |
| $H^i_{\text{eqv}}$ | equivalent inertia constant of all coherent parallel operating unit of the $i$th area (s) |
| $F_{\text{HP}i}$, $F_{\text{IP}i}$ and $F_{\text{LP}i}$ | power fractions of high-, intermediate- and low-pressure turbines of the $i$th area |
| $T_{\text{CH}i}$, $T_{\text{RH}i}$ and $T_{\text{CO}i}$ | time constants of steam chest, reheater and cross-over piping of the $i$th area |
| $a_{ij}$ | area's capacity ratio $(-P_{\text{r}i}/P_{\text{r}j})$ |
| $B_i$ | frequency bias constant of the $i$th area (in pu MW/Hz) |
| $\Delta P_{\text{d}i}$ | step load perturbation of the $i$th area (in pu) |
| $G_{\text{non-reheat}}(s)$ | equivalent transfer function of non-reheat turbine |
| $G_{\text{reheat}}(s)$ | equivalent transfer function of reheat turbine |

## 1 Introduction

To operate the system economically and reliably, the neighbouring power system areas are interconnected through tie-lines. The power exchanges between these areas are frequently scheduled on contract basis via tie-lines named as 'prescheduled interchanges'. The load disturbance in these areas causes the deviations in prescheduled interchanges and system frequency. The automatic generation control (AGC) is used to maintain these prescheduled interchanges and system frequency to their nominal values. The AGC system is divided into two control loops named as primary and secondary control loops. Primary control loop chases the power system load continuously using speed-governing action. However, the system frequency settles down at a new equilibrium point. The secondary control loop helps to restore the system frequency to its initial value. The preliminary studies on AGC system were conducted on tie-line power and frequency control of electric power system. The dynamic performance of AGC system was investigated under the variation of different system parameters: namely, tie-line power controller gains, frequency controller gains, speed regulation parameter, changing tie-line capacity [1, 2] etc. The detailed mathematical modelling of interconnected AGC system was presented and classical control theory had been used first time to optimise the controller gains [3]. Later, state space model of AGC system was also developed and optimal control theory had been utilised to obtain the optimum gain settings [4]. The studies were also conducted on multi-areas interconnected thermal power systems in the presence of governor dead-band effects, generation rate constraints [5, 6]. Furthermore, the study was carried out in discrete mode of AGC system. The secondary control loop consists of supplementary controllers which are updated with the power system data information in every 2 s time interval [7–9]. Supplementary controller chases the area control error signal continuously and tries to diminish it. However, this leads to continuous movement of governor control valve which eventually results to excessive wear and tear of steam turbines. To avoid this difficulty, AGC controller is operated in discrete mode. The control signals are fed to the controllers after a fixed interval of time known as sampling period of the controller. Various intelligent control techniques have been developed to optimise the supplementary controller gains [10–16]. The studies are further extended to the thermal power systems operating at different generation schedules of the plants. The power system load changes considerably over the period of 24 hrs and accordingly the thermal power plants are scheduled to operate at different generation levels. The literature survey shows that the AGC power system model parameters which are considered to be changed along with the generation schedules of the plants are the power system rotating mass time constant $T_{\text{p}}$, power system gain constant $K_{\text{p}}$ and bias factor $B_i$ [17–21]. However, it has been found that these

This is an open access article published by the IET under the Creative Commons Attribution License (http://creativecommons.org/licenses/by/3.0/)

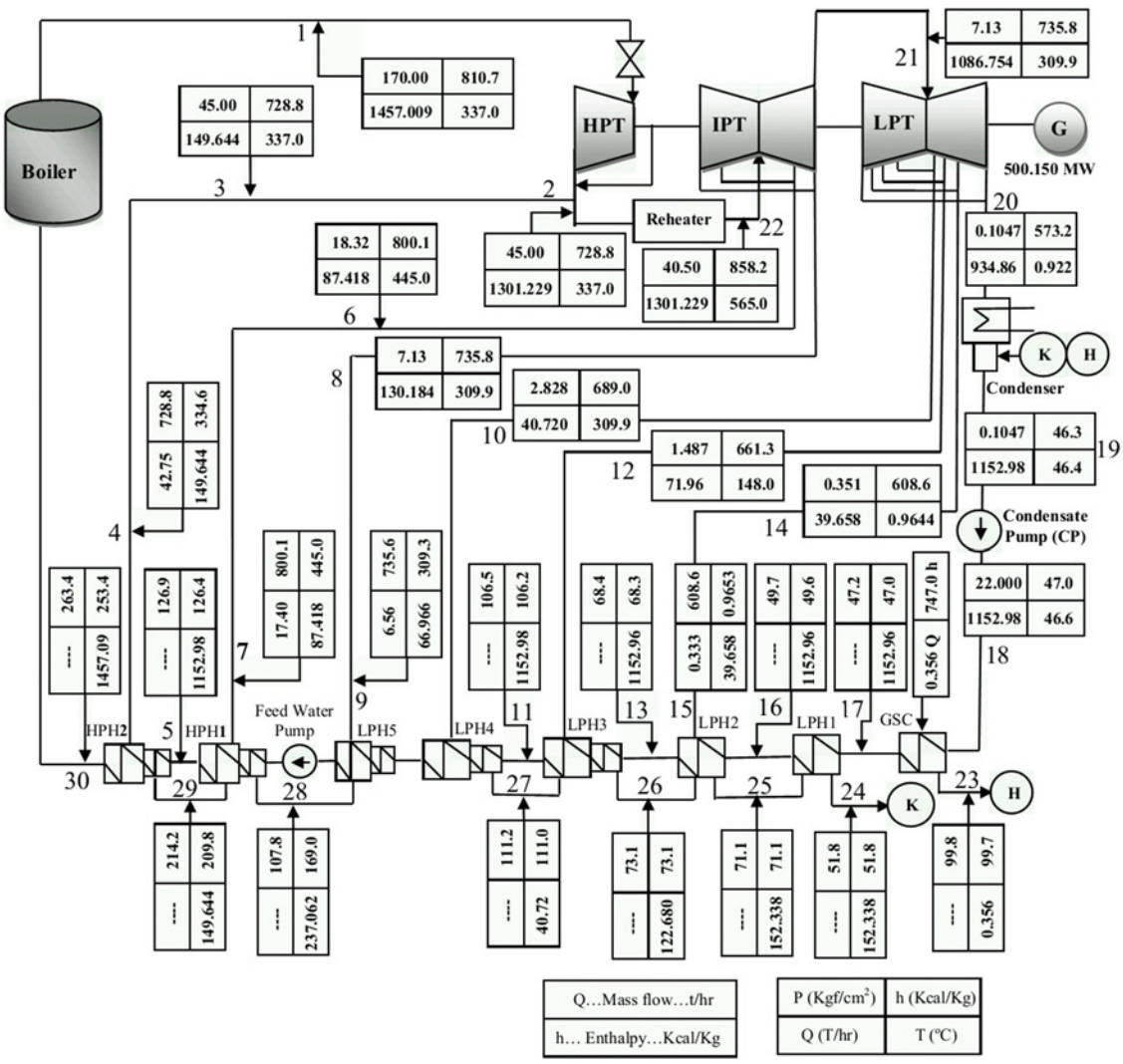


**Fig. 1** *Heat balance diagram of 500 MW unit of thermal power plant for rated power output condition*

system parameters are barely able to affect the power system dynamic response at different generation schedules of the plant. Typically, the generation level of a plant is controlled using one of the following control strategies: constant pressure mode, sliding pressure mode or hybrid mode [22–25]. Mostly hybrid mode, which is the combination of constant pressure and sliding pressure mode is adopted. The steam turbine dynamic model parameters depend on the type of control strategy used to change the generation level of the plant. In the subsequent AGC studies, different kinds of steam turbine dynamic models are used depending on the type of steam turbines being employed in thermal power plants. The IEEE committee taskforce has developed a variety of approximate linear models for all kinds of steam turbines available in thermal power plants [26]. The main parameters of steam turbine dynamic models which describe the dynamics of steam turbines are the time constants of steam chest (SC) $T_{SC}$, reheater (RH) $T_{RH}$, cross-over (CO) $T_{CO}$ and power fractions $F_{HP}$, $F_{IP}$ and $F_{LP}$.

The literature survey shows that either primary/secondary control loops are the main focus areas of the researchers for the AGC dynamics study. Surprisingly, no one has paid attention on the changing dynamic behaviour of steam turbine dynamic model parameters along with the generation schedule of thermal power plant. The previous AGC studies reveal that steam turbine model parameters are assumed to be fixed irrespective of generation schedules of the plant. However, it is discovered that steam turbine dynamic model parameters also change as the generation schedules drifts from its nominal value. Therefore, the dynamic responses and inferences drawn in the preceding AGC studies, assuming the steam turbine dynamic model parameters constant are in doubt. Also, the optimum gain settings of the controllers obtained assuming the steam turbine dynamic model parameters constant may not be acceptable at different generation schedules of the plant.

In this paper, steam turbine dynamic model parameters have been computed for an actual thermal unit of 500 MW capacity, at different power generation schedules of power plant. These computed steam turbine dynamic model parameters have been used to study the dynamic performance of AGC system under varying generating schedule condition. This paper also presents the general mathematical procedure to extract the steam turbine dynamic model parameters from an actual power generating unit. From the literature review, it is observed that there is no mathematical procedure presented yet to compute the steam turbine dynamic model parameters. Hence, in this paper the mathematical procedure is developed to compute these parameters using heat balance data of thermal power plant.

## 2 Thermal power plant cycle with heat balance data

The complete steam cycle of a thermal generating unit of 500 MW capacity has been presented with its heat balance data for rated output condition as shown in Fig. 1. The heat balance data for partial generation levels have been given in Tables 9 and 10 of Appendix 2. The main components of steam units of a thermal power plant are RH, boiler, condensers, turbine sections, feed


This is an open access article published by the IET under the Creative Commons Attribution License (http://creativecommons.org/licenses/by/3.0/)

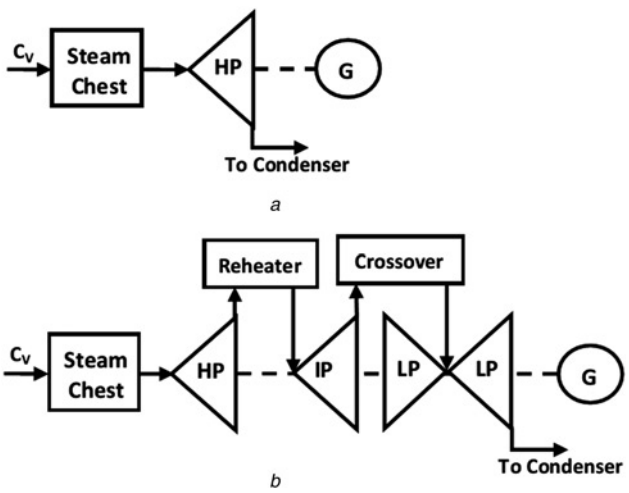


**Fig. 2** *Steam turbine configurations*
*a* Non-reheat turbine
*b* Tandem compound single reheat turbine

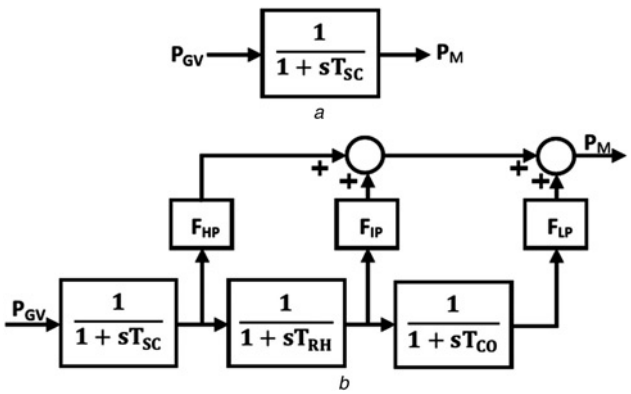


**Fig. 3** *Steam turbine dynamic model of*
*a* Non-reheat steam turbine
*b* Reheat tandem compound steam turbine

water heaters, feed water pumps (FWPs) etc. The steam cycle consists of two high-pressure heaters (HPH) for high pressure turbine (HPT) denoted by HPH1 and HPH2, five low pressure heaters (LPH) for intermediate and lower-pressure turbines denoted by LPH1, LPH2, LPH3, LPH4 and LPH5, respectively. The boiler converts the water into high temperature and pressure steam using constant pressure heating process. At high pressure (HP) and temperature, steam passes through the main control valves and enters into HP steam turbine. Furthermore, it passes through intermediate-pressure turbine (IPT) and low pressure turbine (LPT) and at last reaches to the condenser. The steam may be drained into heat regenerative cycle of feed water heaters when it passes through HPT, IPT and LPTs. The condensate pump pumps the condensate water into the heat regenerative cycle. Before heading toward the steam generator, condensed steam passes through the gland steam condenser, HP and LP heaters, FWP etc. It is important to consider the dynamics of control valve system, turbines, SC, RH and CO for the power system dynamic stability analysis. The other components of the power plant are likely being effective for long-term stability analysis. These turbines generate the mechanical output power which is further transformed into electrical output power using synchronous generators. Furthermore, detailed information about heat balance diagrams is available online on websites of thermal power plants [27]. The comprehensive study of complete steam cycle and heat balance diagram has been carried out in [24, 28].

## 3 Steam turbine dynamic model parameter calculations for power system dynamic studies

The functional block diagrams of non-reheat and reheat steam turbines are shown in Figs. 2*a* and *b*, respectively. The model consists of governor controlled valves (CVs), used to regulate the steam flow at the inlet of HPT. The steam flow cannot change instantly with the change in the CVs position. The steam flow changes with some time lag which is caused by the SC, RH and CO pipes. In the modelling of steam turbine system, these time lags (delays) are incorporated by using time constants for each component causing time lags in the system. The dynamic models of both turbines are shown in Figs. 3*a* and *b*, respectively [26]. The typical parameters of these models are the time constants $T_{SC}$, $T_{RH}$ and $T_{CO}$ of SC, RH, CO pipe and the power fractions $F_{HP}$, $F_{IP}$ and $F_{LP}$ of HP, IP and LPTs, respectively. The transfer function models of non-reheat and single reheat steam turbines derived from Figs. 3*a* and *b* are as follows.

*Equivalent transfer function model of non-reheat turbine*

$$G_{\text{non-reheat}}(s) = \frac{1}{(1 + sT_{SC})} \tag{1}$$

*Equivalent transfer function of reheat tandem compound steam turbine*

$$G_{\text{Reheat}}(s) = \left\{ \left( F_{IP} + \frac{F_{LP}}{(1 + sT_{CO})} \right) \frac{1}{(1 + sT_{RH})} + F_{HP} \right\} \frac{1}{(1 + sT_{SC})} \tag{2}$$

$$G_{\text{Reheat}}(s) = \frac{F_{HP}}{(1 + sT_{SC})} + \frac{F_{IP}}{(1 + sT_{SC})(1 + sT_{RH})} + \frac{F_{LP}}{(1 + sT_{SC})(1 + sT_{RH})(1 + sT_{CO})} \tag{3}$$

$$G_{\text{Reheat}}(s) = \frac{F_{HP}(1 + sT_{RH})(1 + sT_{CO}) + F_{IP}(1 + sT_{CO}) + F_{LP}}{(1 + sT_{SC})(1 + sT_{RH})(1 + sT_{CO})} \tag{4}$$

(see (5))

As the sum of all power fractions is 1 pu, i.e. $F_{HP} + F_{IP} + F_{LP} = 1$. Therefore, $G_{\text{Reheat}}(s)$ can be written as

$$G_{\text{Reheat}}(s) = \frac{1 + (T_{CO}F_{IP} + T_{RH}F_{HP} + T_{CO}F_{HP})s + T_{RH}T_{CO}F_{HP}s^2}{(1 + sT_{SC})(1 + sT_{RH})(1 + sT_{CO})} \tag{6}$$

The methodology for finding the values of these parameters using heat balance diagram are as follows.

### 3.1 Time constant calculation

The steam turbine dynamic model parameters contain the time constants of SC, RH and CO. These time constants can be calculated

$$G_{\text{Reheat}}(s) = \frac{(F_{HP} + F_{IP} + F_{LP}) + (T_{CO}F_{IP} + T_{RH}F_{HP} + T_{CO}F_{HP})s + T_{RH}T_{CO}F_{HP}s^2}{(1 + sT_{SC})(1 + sT_{RH})(1 + sT_{CO})} \tag{5}$$

This is an open access article published by the IET under the Creative Commons Attribution License (http://creativecommons.org/licenses/by/3.0/)

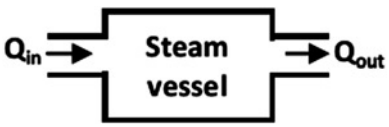


**Fig. 4** *Steam vessel containing inlet and outlet ports for steam passage*

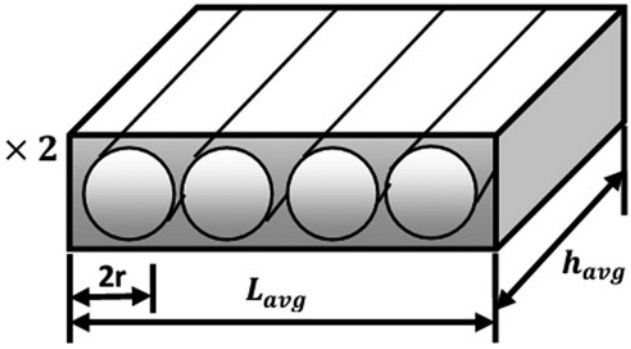


**Fig. 5** *Reheater configuration of the thermal power plant*

using the expression derived for the calculation of steam vessel's time constant as shown in Fig. 4. This expression derived using the mass continuity equation is given as [29, 30]

$$T_{\mathrm{V}} = \frac{P_o}{Q_o} V_{\mathrm{vessel}} \times K_{\mathrm{vessel}} \tag{7}$$

where

$$K_{\mathrm{vessel}} = \left.\frac{\partial \rho}{\partial P}\right|_{T\,(^\circ\mathrm{C})} \tag{8}$$

where $T_{\mathrm{V}}$ is the vessel steam flow time constant in seconds, $Q_o$ is the vessel's steam flow rate in kilograms/seconds, $P_o$ is the steam pressure in vessel, $V_{\mathrm{vessel}}$ is the volume of vessel and $K_{\mathrm{vessel}}$ is the change in steam density with respect to change in pressure at a particular temperature. The pressure, flow and temperature can be obtained using heat balance diagram of thermal power plant. The $K_{\mathrm{vessel}}$ can be calculated from the available thermodynamic data of steam table [31]. It is important to know that the temperatures at which we want to find the thermodynamic data sometimes may not be given in the steam table. The linear interpolation technique is generally used to approximate the data of steam for the temperatures not available in the steam table. Equations (7) and (8) can be used to find the time constants of SC, RH and CO.

### 3.2 *Power fraction calculation*

The power fractions determine the proportion of total power produced by HP, IP and LP steam turbines. Assuming, the total power shared by these turbines has been represented on unit base. It can be written as

$$F_{\mathrm{HP}} + F_{\mathrm{IP}} + F_{\mathrm{LP}} = 1 \tag{9}$$

These power fractions in terms of power output can be written as

$$\frac{F_{\mathrm{LP}}}{F_{\mathrm{HP}}} = \frac{P_{\mathrm{LP}}}{P_{\mathrm{HP}}} = a_1 \tag{10}$$

and

$$\frac{F_{\mathrm{IP}}}{F_{\mathrm{HP}}} = \frac{P_{\mathrm{IP}}}{P_{\mathrm{HP}}} = a_2 \tag{11}$$

where $P_{\mathrm{HP}}$, $P_{\mathrm{IP}}$ and $P_{\mathrm{LP}}$ are the power outputs of HP, IP and LP steam turbines. The turbine power outputs can be obtained by using the enthalpy and steam flow data available in the heat balance diagram. The power output can be obtained using the following equation

$$P_X = \sum_{k=1}^{n} Q_k (h_{\mathrm{in},k} - h_{\mathrm{out},k}) \tag{12}$$

where $P_X$ is the output power and $X$ stands for HPT, IPT or LPTs, $k$ = indices of turbine stage between draining points, in kilojoules/seconds, $Q_k$ is the flow rate of the $k$th stage, $h_{\mathrm{in},k}$ and $h_{\mathrm{out},k}$ are the inlet and outlet enthalpies of the $k$th stage. From (10)–(12), power fractions can be written as

$$F_{\mathrm{HP}} = \frac{1}{1 + a_1 + a_2},\ F_{\mathrm{IP}} = \frac{a_2}{1 + a_1 + a_2} \text{ and } F_{\mathrm{LP}} = \frac{a_1}{1 + a_1 + a_2} \tag{13}$$

The values of $a_1$ and $a_2$ are calculated assuming that the process is isentropic and the losses (mechanical) are ignored.

## 4 Evaluation of steam turbine model parameters for different generation schedules of thermal plant

The 500 MW unit of thermal power plant has been considered for the calculation of steam turbine model parameters. The complete heat balance diagram of the plant is shown in Fig. 1, which represents the rated generation regime. The heat balance data for partial generation schedule is not shown in this figure, instead it has been tabulated in Tables 9 and 10 of Appendix 2. The heat balance diagram consists of pressure, enthalpy, mass flow rate and temperature of various components and pipe sections of plant cycle. The calculations of parameters of steam turbine dynamic model

**Table 1** Calculated values of time constant and heat balance data for steam chest at different generation schedules

| 0% make up (MU) 0.1047 at back pressure | | | | | |
|---|---|---|---|---|---|
| Generation schedules, % | Pressure, kgf/cm$^2$ | Enthalpy, kcal/kg | Flow, t/h | Temperature, °C | $T_{\mathrm{SC}}$, s |
| 100 | 170 | 810.7 | 1457.009 | 537 | 0.2990 |
| 80 | 170 | 810.7 | 1166.642 | 537 | 0.3746 |
| 60 | 170 | 810.7 | 887.632 | 537 | 0.4922 |
| 50 | 170 | 810.7 | 755.373 | 537 | 0.5786 |
| 30 | 170 | 783.2 | 552.646 | 497 | 0.8947 |


This is an open access article published by the IET under the Creative Commons Attribution License (http://creativecommons.org/licenses/by/3.0/)

**Table 2** Calculated values of time constant and heat balance data for reheater at different generation schedules

| 0% MU 0.1047 at back pressure | | | | | | |
|---|---|---|---|---|---|---|
| Generation schedules, % | Pressure, kgf/cm$^2$ | Enthalpy, kcal/kg | Flow, t/h | Input temperature, °C | Output temperature, °C | $T_{RH}$, s |
| 100 | 40.5 | 858.2 | 1301.229 | 337 | 565 | 5.00 |
| 80 | 32.81 | 859.8 | 1051.583 | 337 | 565 | 5.01 |
| 60 | 25.26 | 861.4 | 808.262 | 337 | 565 | 5.02 |
| 50 | 20.61 | 862.4 | 656.828 | 337 | 565 | 5.04 |
| 30 | 12.98 | 815.6 | 437.216 | 437.21 | 472 | 5.37 |

**Table 3** Calculated values of time constant and heat balance data for cross-over at different generation schedules

| 0% MU 0.1047 at back pressure | | | | | | |
|---|---|---|---|---|---|---|
| Generation schedules, % | Pressure, kgf/cm$^2$ | Enthalpy, kcal/kg | Flow, t/h | Temperature, °C | $\frac{\partial\rho}{\partial P}$, s$^2$/m$^2$ | $T_{CO}$, s |
| 100 | 7.13 | 735.8 | 1086.754 | 309.9 | 0.003839 | 0.4000 |
| 80 | 5.80 | 737.2 | 883.566 | 311.4 | 0.003790 | 0.3970 |
| 60 | 4.49 | 738.6 | 680.817 | 312.8 | 0.003770 | 0.3966 |
| 50 | 3.91 | 742.3 | 589.281 | 319.5 | 0.003715 | 0.3932 |
| 30 | `2.74 | 714.6 | 424.432 | 261.2 | 0.004125 | 0.4248 |

**Table 4** Calculated values of MW outputs for HP, IP and LP turbines at different generation schedules

| Generation schedule, % | $P_{HP}$, MW | $P_{IP}$, MW | $P_{LP}$, MW | $P_T$, MW | $P_{loss}$, MW | $P_{net}$, MW |
|---|---|---|---|---|---|---|
| 100 | 138.864 | 178.837 | 191.439 | 509.173 | 9.173 | 500 |
| 80 | 110.646 | 144.895 | 151.382 | 406.923 | 6.923 | 400 |
| 60 | 83.5652 | 111.712 | 110.9735 | 306.25 | 6.250 | 300 |
| 50 | 73.4910 | 96.9823 | 85.4160 | 255.89 | 5.890 | 250 |
| 30 | 50.9830 | 59.1584 | 44.3843 | 154.5415 | 4.5415 | 150 |

using heat balance diagram of thermal power plant are in Section 4.1. The conversion factors used in the calculations are as follows: 1 kgf/cm$^2$ = 98.0665 kPa, 1 t/h = 0.277778 kg/s and 1 kcal/kg = 4.186 kJ/kg.

### *4.1 Calculation of time constants for different generation schedules*

*4.1.1 Steam chest time constant:* The average radius and height of the SC cylinder are $r_{avg} = 67.2$ cm and $h_{avg} = 150$ cm. The volume of cylinder is given as $V_{SC} = \pi h_{avg} r_{avg}^2 = 2.1298$ m$^3$. The thermodynamic data of SC extracted from the heat balance diagram is shown in Table 1. Here, SC time constant calculations are shown only for rated power output condition. The same procedure can be used for partial generation levels/schedules also. From the heat balance diagram rated pressure and flow of SC are as follows: $P_{SC} = 170 \times 98.0665 = 16671.305$ kPa, $Q_{SC} = 1457.009 \times 0.278 = 405.04$ kg/s. The pressure–density curve derived from the steam table [31], using simple curve fitting technique is given as

$$\rho(p) = C_{SC1} + C_{SC2} \cdot p + C_{SC3} \cdot p^2 + C_{SC4} \cdot p^3 \text{ kg/m}^3, \text{ for } 13,000 \le P \le 17,000 \text{ kPa at } 537^\circ\text{C} \quad (14)$$

All the coefficient values of $C_{SC1}$, $C_{SC2}$, $C_{SC3}$ and $C_{SC4}$ are given in Appendix 1. Differentiating (14), with respect to pressure ($p$) gives

$$\frac{\partial\rho}{\partial P} = C_{SC2} + 2.C_{SC3}.\, p + C_{SC4}.\, p^2 \text{ s}^2/\text{m}^2, \quad (15)$$

**Table 5** Power fractions of HP, IP and LP turbines for different generation schedules

| Generation schedule, % | $F_{HP}$ | $F_{IP}$ | $F_{LP}$ |
|---|---|---|---|
| 100 | 0.2727 | 0.3511 | 0.3760 |
| 80 | 0.2719 | 0.3560 | 0.3720 |
| 60 | 0.2728 | 0.3647 | 0.3623 |
| 50 | 0.2872 | 0.3790 | 0.3338 |
| 30 | 0.3299 | 0.3828 | 0.2872 |

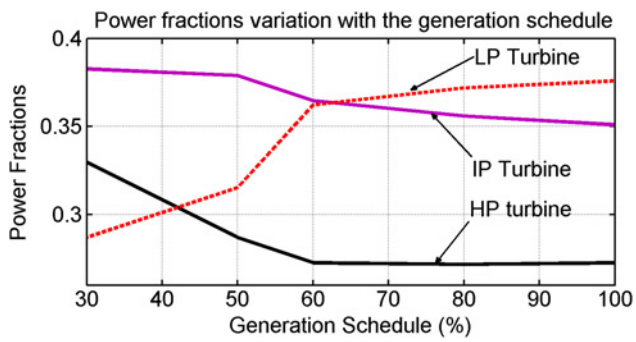


**Fig. 6** *Power fractions variation along with the generation schedule of the plant*

This is an open access article published by the IET under the Creative Commons Attribution License (http://creativecommons.org/licenses/by/3.0/)

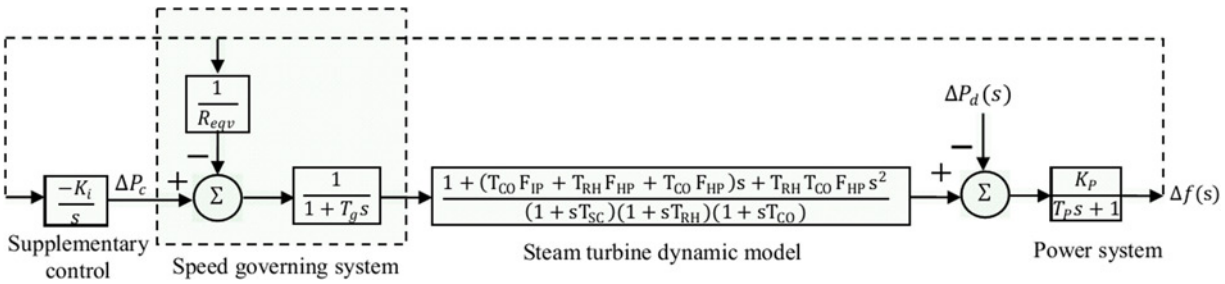


**Fig. 7** *Transfer function model of single area AGC system with reheat steam turbine dynamic model*

$$\left.\frac{\partial\rho}{\partial P}\right|_{\substack{537^\circ\mathrm{C},\\ 16671.305\,\mathrm{kPa}}} = 0.00341\,\mathrm{s}^2/\mathrm{m}^2, \tag{16}$$

The time constant ($T_{SC}$) of SC is

$$T_{sc} = \frac{P_{SC}}{Q_{SC}} V_{SC} \frac{\partial\rho}{\partial P} = 0.2999\,\mathrm{s} \tag{17}$$

Similarly, time constant can be calculated for different generation schedules by extracting the heat balance data. All calculated values of SC time constants for rated and partial generation schedules have been tabulated in Table 1.

*4.1.2 Reheater time constant:* Generally, RHs are double pipe set structures and are located between HPT and LPTs and usually buildup on the furnace heating walls. Fig. 5 shows a simple design of RH used in the plant. The average height, radius and length are taken as follows: $H_{avg} = 12$ m, $r_{avg} = 47.86$ cm and $L_{avg} = 8$ m. The volume of the RH can be approximated as $V_{RH}$ = number of rows × number of pipes in a single row × volume of a single pipe. Thus, RH volume is given as $V_{RH} = 2 \times (L_{avg}/2r) \times \pi \cdot r^2 \cdot H_{avg} = \pi \cdot r \cdot H_{avg} \cdot L_{avg} = 144.36\,\mathrm{m}^3$. Here, two rows of pipes are considered because of the fact that the plant RH has the double pipe set arrangement. The spacing between the pipes has been neglected.

From the heat balance diagram, $P_{RH} = 40.5 \times 98.0665 = 3971.69325$ kPa, $Q_{RH} = 1301.229 \times 0.278 = 361.741$ kg/s. It is clear from Table 1, i.e. temperature of the RH increases from 337 to 565°C. Therefore, approximated time constant can be calculated by taking the average temperature given as $T_{avg} = ((337 + 565)/2) = 451^\circ$C. The pressure–density curve derived from the steam table [31], using simple curve fitting technique is given in (18). The coefficient values of $C_{RH1}$, $C_{RH2}$, $C_{RH3}$ and $C_{RH4}$ are given in Appendix 1

$$\rho(p) = C_{RH1} + C_{RH2} \cdot p + C_{RH3} \cdot p^2 + C_{RH4} \cdot p^3 \quad \text{for} \quad 3800 \le P \le 4200\,\text{kPa at } 451^\circ\text{C} \tag{18}$$

$$\frac{\partial\rho}{\partial P} = C_{RH2} + 2 \cdot C_{RH3} \cdot p + C_{RH4} \cdot p^2\,\mathrm{s}^2/\mathrm{m}^2, \tag{19}$$

$$\left.\frac{\partial\rho}{\partial P}\right|_{\substack{451^\circ\mathrm{C},\\ 3971.69\,\mathrm{kPa}}} = 0.0031544\,\mathrm{s}^2/\mathrm{m}^2, \tag{20}$$

The time constant ($T_{RH}$) of RH is

$$T_{RH} = \frac{P_{RH}}{Q_{RH}} V_{RH} \frac{\partial\rho}{\partial P} = 5.00\,\mathrm{s} \tag{21}$$

Similarly, RH time constants can be calculated for partial generation schedules. All calculated values of RH time constants for rated and part generation schedules have been tabulated in Table 2.

*4.1.3 Cross-over time constant:* The CO pipe is located between IPT and LPTs. The dimensions are radius $r = 130.14$ cm and

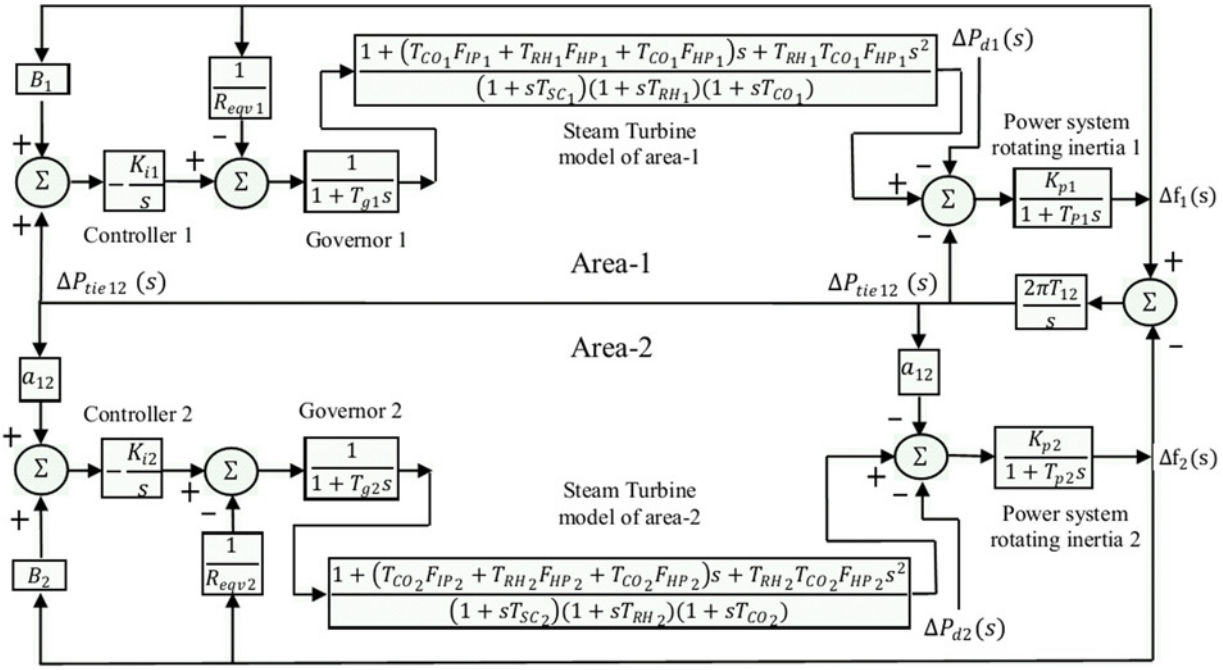


**Fig. 8** *Transfer function block diagram of thermal–thermal power system model*


This is an open access article published by the IET under the Creative Commons Attribution License (http://creativecommons.org/licenses/by/3.0/)

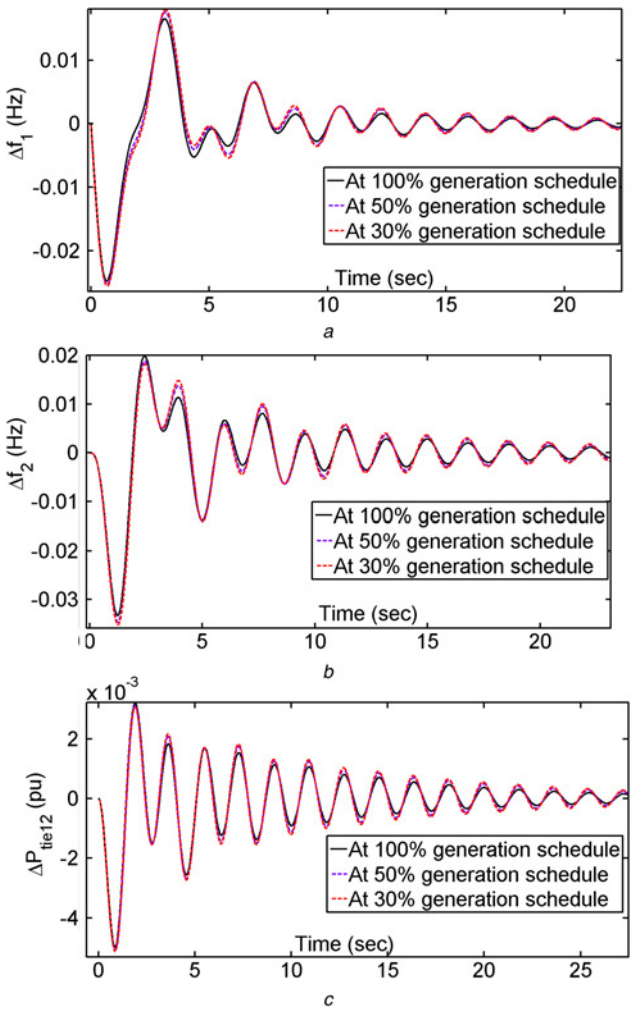


**Fig. 9** *Dynamic responses of the system at different generation schedules assuming the steam turbine model parameters constant irrespective of generation schedules of the plant*
*a* Frequency deviation of area-1
*b* Frequency deviation of area-2
*c* Tie-line power deviation

length $L_{avg} = 8.5$ m. The volume of the CO is $V_{CO} = \pi \cdot r^2 \cdot L_{avg} = 45.23\ m^3$. From the heat balance diagram, $P_{RH} = 7.13 \times 98.0665 = 699.214$ kPa and $Q_{RH} = 1086.754 \times 0.278 = 302.117$ kg/s. The pressure–density curve derived from the steam table [31] using simple curve fitting technique is given below. The coefficient values of $C_{Co1}$, $C_{Co2}$, $C_{Co3}$ *and* $C_{Co4}$ are given in Appendix 1

$$\rho(p) = C_{Co1} + C_{Co2} \cdot p + C_{Co3} \cdot p^2 + C_{Co4} \cdot p^3, \quad \text{for } 400 \le P \le 1000\,\text{kPa at } 451^\circ\text{C} \tag{22}$$

$$\frac{\partial \rho}{\partial P} = C_{Co2} + 2 \cdot C_{Co3} \cdot p + C_{Co4} \cdot p^2, \tag{23}$$

$$\left.\frac{\partial \rho}{\partial P}\right|_{\substack{309.9^\circ\text{C},\\ 699.214\,\text{kPa}}} = 0.003839\ \text{s}^2/\text{m}^2, \tag{24}$$

The time constant ($T_{CO}$) of CO is

$$T_{CO} = \frac{P_{CO}}{Q_{CO}} V_{CO} \frac{\partial \rho}{\partial P} = 0.400\ \text{s} \tag{25}$$

Similarly, CO time constants can be calculated for partial generation schedules as shown in Table 3.

### 4.2 *Calculation of HPT, IPT and LPT power fractions at different generation schedules of the plant*

The power fractions have been calculated using enthalpy and steam flow data of the plant. The power fraction calculations have been shown only for two cases, i.e. for 100 and 80% generation schedule of the plant as given in Appendix 3. The values of $a_1$ and $a_2$ are calculated using (10) and (11), then the power fractions are calculated using (12) and (13). The same procedure can be used to calculate the power fractions at other power generation schedules. All calculated values of megawatt outputs and power fractions of HPT, IPT and LPTs for different generation schedules have been tabulated in Tables 4 and 5, respectively.

The power fractions variation of reheat turbine system along with generation schedule of the plant is shown in Fig. 6. It is very interesting to know that at rated power output HPT, IPT and LPTs are contributing 27, 35 and 38% of total power output, respectively. As the generation schedule decreases, LPT contribution in total power output decreases while the HPT and LPTs contribution increases. At 30% generation schedule HPT, IPT and LPTs contributions are 32, 39 and 29% which means that LPT contribution has been decreased by 9% while HPTs and IPTs contributions have been increased by 5 and 4%, respectively. Hence, the power fractions of HPT, IPT and LPTs are varying considerably with the generation schedule of the plant. The power fraction values used at rated power generation are no longer valid for partial generation schedules and needs to be recalculated in studying the dynamic performance of the AGC system.

## 5 Simulation results and discussion

The two areas of thermal power system have been considered for the investigation. The area-1 consists of four parallel units, each of 500 MW capacities and having the total generating capacity of $4 \times 500$ MW = 2000 MW. The area-2 is having the two parallel units of 500 MW, having the total generating capacity of $2 \times 500$ MW = 1000 MW. Identical steam turbines have been employed in both areas; therefore, same heat balance data have been used to evaluate the turbine model parameters of all steam turbines of both power system areas. The unit size is taken as 500 MW just for the purpose of demonstration of the concept. However, the methodology is general enough and can be applied to any other system also.

It is assumed that all generating units in each area swings coherently. Therefore, all parallel operating units in their respective areas can be replaced by a single generating unit having equivalent inertia constant. For a system of '$n$' generating units operating in parallel coherently having inertia constants $H_1$, $H_2$, $H_3$… and ratings $S_1$, $S_2$, $S_3$…. Then equivalent inertia constant $H_{eqv}$ of all generating units can be written as [32]

$$H_{eqv} = \frac{H_1 S_1 + H_2 S_2 + \ldots + H_n S_n}{H_{system}}\ \text{s}, \tag{26}$$

where

$$H_{system} = H_1 + H_2 + \ldots + H_n. \tag{27}$$

Using (26) and (27), power system rotating mass time constant $T_P$ and power system gain $K_p$ can be calculated as follows

$$T_P = \frac{2H_{eqv}}{D \cdot f}\ \text{s},\ K_p = \frac{1}{D}\ \text{Hz/Mw pu}. \tag{28}$$

The power system frequency characteristic depends on the combined effect of speed droops of all generator speed governors. For a system of '$n$' generating units having droops $R_1$, $R_2$, $R_3$… and composite load damping constant $D$, the steady-state frequency

This is an open access article published by the IET under the Creative Commons Attribution License (http://creativecommons.org/licenses/by/3.0/)

**Table 6** System parameter values at different generation schedules of the plant assuming steam turbine model parameters constant

| Total load, MW | Generation schedules, % | Area-1 | | | | Area-2 | | | |
|---|---|---|---|---|---|---|---|---|---|
| | | MW output | $T_{P1}$, s | $K_{p1}$ | $B_1$ | MW output | $T_{P2}$, s | $K_{p2}$ | $B_2$ |
| 3000 | 100 | 2000 | 10 | 60 | 0.433 | 1000 | 10 | 60 | 0.433 |
| 1500 | 50 | 1000 | 20 | 120 | 0.425 | 500 | 20 | 120 | 0.425 |
| 900 | 30 | 600 | 33.3 | 200 | 0.422 | 300 | 33.3 | 200 | 0.422 |

**Table 7** Optimised controller gains at different generation schedules of the plant assuming steam turbine model parameters constant

| Generation schedules, % | Controller gains | |
|---|---|---|
| | $K_{i1}$ | $K_{i2}$ |
| 100 | 1.723 | 0.320 |
| 50 | 1.627 | 0.283 |
| 30 | 1.582 | 0.269 |

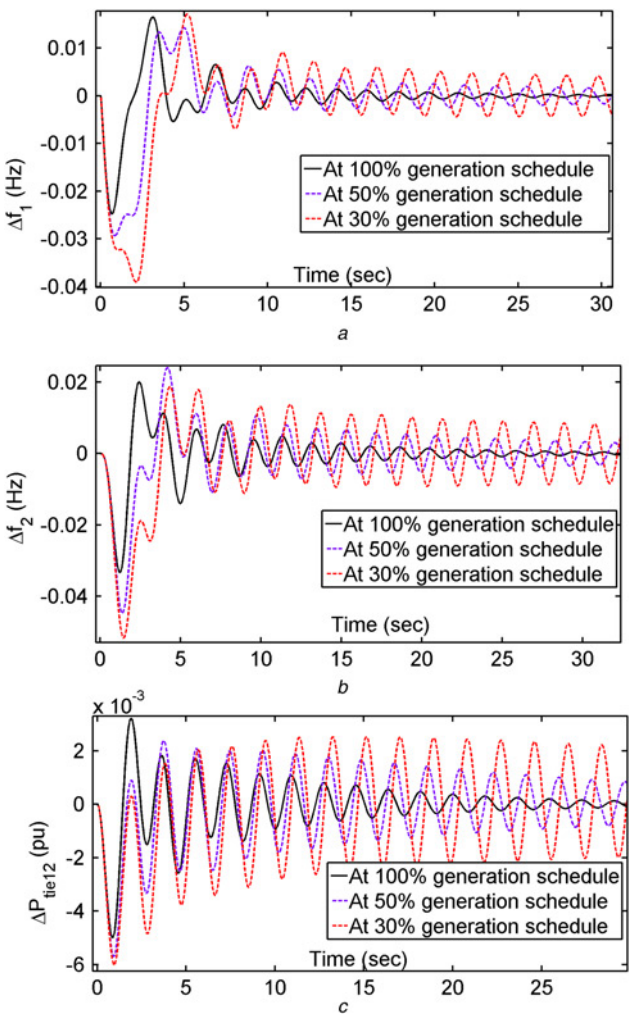


**Fig. 10** *Dynamic response of the system at different generation schedules after considering the variation of steam turbine time constant along with generation schedules of the plant*
*a* Frequency deviation of area-1
*b* Frequency deviation of area-2
*c* Tie-line power deviation

deviation for a load disturbance of $\Delta P_{\mathrm{d}}$ is given as [30]

$$\Delta f_{ss} = \frac{-\Delta P_{\mathrm{d}}}{(1/R_1 + 1/R_2 + \ldots 1/R_n) + D}\ \mathrm{Hz} \tag{29}$$

$$\Delta f_{ss} = \frac{-\Delta P_{\mathrm{d}}}{\left(1/R_{\mathrm{eqv}}\right) + D}\ \mathrm{Hz} \tag{30}$$

where

$$R_{\mathrm{eqv}} = \frac{1}{(1/R_1 + 1/R_2 + \ldots + 1/R_n)}\ \mathrm{Hz/MW\,pu.} \tag{31}$$

The parameters $R_{\mathrm{eqv}}$, $T_{\mathrm{P}}$ and $K_{\mathrm{P}}$ are calculated using above equations are given in Table 11 of Appendix 4. It is found that the equivalent inertia constant and speed regulation parameter of all generating units based on system rating (total area capacity) are same as the values of inertia constant and speed regulation parameter of a single unit based on its own individual rating. On the basis of (26)–(31), the equivalent block diagram of single area AGC system consisting '$n$' generating units has been drawn in Fig. 7. Block diagram includes the equivalent speed-governing system, steam turbine dynamic model and rotating mass and load suitable for load frequency analysis. The steam turbine model used in diagram is based on (6), derived for reheat steam turbine. To obtain the transfer function of non-reheat turbine, simply put $T_{\mathrm{RH}}$ and $T_{\mathrm{CO}}$ equals to zero. The transfer function block diagram of two area interconnected power system is shown in Fig. 8. System parameter values are given in Appendix 4. The dynamic responses have been obtained for 1% load perturbation in area-1 at different generation schedules of the thermal power plant. The supplementary controller gains have been optimised based on integral squared error (ISE) optimisation criterion given as

$$J = \int_0^T \left(\left|\Delta f_1(\mathrm{s})\right|^2 + \left|\Delta P_{\mathrm{tie}\,12}(\mathrm{s})\right|^2\right) \mathrm{d}t \tag{32}$$

where '$T$' is the total simulation time. The classical control algorithm has been used for the tuning of controller gains. In this approach sequential optimisation is adopted where one parameter is optimised at a time, keeping other parameters fixed using ISE

**Table 8** Optimised controller gains at different generation schedules of the plant considering the variation of steam turbine model parameters along with generation schedules

| Generation schedules, % | SC time constant ($T_{t1}$ and $T_{t2}$), s | Controller gains | |
|---|---|---|---|
| | | $K_{i1}$ | $K_{i2}$ |
| 100 | 0.2999 | 1.732 | 0.320 |
| 50 | 0.5786 | 0.618 | 0.73 |
| 30 | 0.8947 | 0.301 | 0.086 |


This is an open access article published by the IET under the Creative Commons Attribution License (http://creativecommons.org/licenses/by/3.0/)

criterion. The process is repeated for other parameters until optimum value is reached. This method is suitable for cases where the numbers of optimisation variables are less; otherwise, heuristic algorithms are used. However, in this case there are only two variables to optimise; therefore, classical control approach will be self-sufficient to optimise the controller gains.

Here, two cases have been studied. In the first case, the dynamic responses of the system have been obtained at different generation schedules assuming the steam turbine model parameters constant irrespective the generation schedules of the plant. The power system parameters $K_p$, $T_p$ and $B_i$ are only considered to be variable along with the power plant generation schedules. In the second case, steam turbine model parameters are also considered to be varying with the plant generation schedules.

### *5.1 Case-1: Steam turbine dynamic model parameters are assumed to be constant irrespective to the generation schedules of the plant*

In this case, steam turbine dynamic model parameters are assumed to be fixed. Only power system model parameters $K_p$, $T_p$ and $B_i$ are considered to be variable along with generation schedules. Frequency and tie-line power deviations of power system are shown in Fig. 9. It is found that the dynamic response of the system almost remains same at all generation schedules of the plant. Though the power system parameters $K_p$, $T_p$ and $B_i$ are changing with the generation schedules, still they are barely able to affect the dynamic responses of the system. The power system model parameter values and optimum controller gain settings for different generation schedules of the plant have been presented in Tables 6 and 7, respectively. It is also clear for Table 7, i.e. controller gain settings are also slightly affected by the generation schedules of the plant.

### *5.2 Case-2: Steam turbine dynamic model parameters are considered to be varying along with the generation schedules of the plant*

In this case, steam turbine model parameters are also considered to be variable along with the generation schedule of the plant. The power system dynamic responses are shown in Fig. 10. It is clear from figure that as the generation schedule of the plant drifts down from the plant's rated output; the dynamic responses of the system becoming more oscillatory in nature, i.e. number of oscillations and settling time are increasing considerably. The first peak of oscillation has been increased considerably at 30% generation schedule of the plant. It is happening due to the fact that the steam turbine time constant is increasing as the generation schedule is shifting downwards from the rated value. After comparing Figs. 9 and 10 of cases 1 and 2, respectively, it is also clear that the steam turbine dynamic model parameters are dominating over the power system parameters in deciding the dynamic performance of the system, as the power system parameters $K_p$, $T_p$ and $B_i$ are hardly able to affect the dynamic response of the system, while the steam turbine model parameters variation with the generation schedules of the plant making the system more oscillatory. The optimum gain settings of the controllers of the thermal power system model are presented in Table 8, for different generation schedules of the plant. It can be seen from this table that the controller gain settings are also changing considerably with generation schedule of the plant. The optimum gain settings used at 100% generation scheduling are no longer valid at partial scheduling of the plant and needs to be recalculated.

Hence, it can be concluded that in AGC studies, the variation steam turbine model parameters along with plant generation schedules should be considered in order to get more realistic response of the system. The dynamic responses obtained while keeping the turbine model parameters constant in such studies are very far from the actual responses of the system.

## 6 Conclusions

Dynamic performance of AGC system has been studied at different generation schedules. The AGC performance very much relies on the steam turbine dynamic model parameters. The steam turbine model parameters are found to be dependent on the generation schedules of thermal power plants. This paper incorporates the effect of steam turbine model parameters variation in the dynamic performance of AGC system. A realistic 500 MW units have been considered for study. Heat balance data is used to extract the steam turbine model parameters at different generation schedules. Some sturdy points have been highlighted which are the main contributions of the work, are as follows:

(i) The IEEE committee has just recommended the values of steam turbine dynamic model parameters; however, it has not been described how to estimate these parameters from a realistic generating unit of thermal power plant. This paper presents the mathematical procedure to calculate the steam turbine model parameters by simply using the heat balance data (most likely available data) of the thermal power plant.

(ii) The IEEE committee has recommended the value of steam turbine (SC) time constant in the range of 0.2–0.5 s and in most of AGC studies 0.3 s has been selected without any justification [1–21]. The committee also did not mention any dependency of the steam turbine time constant on the generation schedule of the plant. However, authors found that the steam turbine time constant depends on the generation schedule of the plant and varies in the range of 0.2–1.0 s, particularly in this case at 30, 50 and 100% generation levels, the calculated values of time constants are 0.8947 s, 0.5786 s and 0.2999 s, respectively. Hence, the range of time constant defined by the IEEE committee needs some modifications. Also, the value of the turbine time constant should be selected based on the generation level of the plant. As we can observe that the value of the steam turbine time constant affects the dynamic performance of the entire thermal power system model; therefore, exact value of the time constant at a particular generation level should be calculated using the mathematical procedure presented in this paper. The RH and CO time constant almost remains the same for all generation levels of the plant. Hence, at partial generation schedules, only SC time constant needs to be recalculated.

(iii) The IEEE committee also recommended the values of steam turbine power fractions only for rated power output condition of the plant. However, it has been discovered that the power fractions of the steam turbines are also varied considerably along with generation schedules of the plant. It has been observed that typically, at 100% loading condition HPT, IPT and LPT shares to the total power outputs are 27, 35 and 38%, respectively. However, at 30% generation level 5% increase in HP, 4% increase in IP and 9% decrease in LPT have been recorded. Hence, in generalised form, it can be stated that as the generation shifts down from its rated value, the power share/fraction of LPT decreases while this share is compensated by the increase of power share/fractions of IP and HP turbines. These power fraction changes must be accounted in the dynamic studies of AGC system. The power fractions at partial generation levels/schedules can be calculated using the method presented in this paper.

(iv) At last, it has been observed that the AGC dynamic performance degrades as the scheduled generation drifts down from rated output of the plant. The steam turbine time constant is the main parameter which deteriorates the dynamic performance of the system. The optimum controller gains obtained for 100% generation schedules are completely unacceptable

This is an open access article published by the IET under the Creative Commons Attribution License (http://creativecommons.org/licenses/by/3.0/)

at partial generation schedules and needs to be recalculated as the generation schedule changes.

## 7 Acknowledgment

Authors want to thank to Mr. Manish Kumar who shared his knowledge and insight work experience and assisted in research work. He is currently working as a Project Engineer in NTPC Ltd. (National Thermal Power Corporation Limited), India.

## 8 References

[1] Concordia C., Kirchmayer L.K.: 'Tie-line power and frequency control of electric power systems', *Power Appar. Syst. III, Trans. Am. Inst. Electr. Eng.*, 1953, **72**, (2), pp. 562–572
[2] Concordia C., Kirchmayer L.K.: 'Tie-line power and frequency control of electric power systems – part II', *Power Appar. Syst. III. Trans. Am. Inst. Electr. Eng.*, 1954, **73**, (1), pp. 133–146
[3] Elgerd O.I., Fosha C.: 'Optimum megawatt frequency control of multi-area electric energy systems', *IEEE Trans. Power Appar. Syst.*, 1970, **PAS-89**, (4), pp. 556–563
[4] Fosha C., Elgerd O.I.: 'The megawatt-frequency control problem: a new approach via optimal control theory', *IEEE Trans. Power Appar. Syst.*, 1970, **PAS-89**, (4), pp. 563–577
[5] Asadur R., Saikia C.L., Nidul S.: 'Maiden application of hybrid pattern search biogeography based optimisation technique in automatic generation control of a multi-area system incorporating interline power flow controller', *IET Gener. Transm. Distrib.*, 2016, **10**, (7), pp. 1654–1662
[6] Chvez H., Baldick R., Matevosyan J.: 'The joint adequacy of AGC and primary frequency response in single balancing authority systems', *IEEE Trans. Sustain. Energy*, 2015, **6**, (3), pp. 959–966
[7] Kumar A., Malik O.P., Hope G.S.: 'Discrete variable structure controller for load frequency control of multi-area interconnected power systems', *IEE Proc. C, Gener. Transm. Distrib.*, 1987, **134**, (2), pp. 116–122
[8] Tripathy S.C., Bhatti T.S., Jha C.S., *ET AL.*: 'Sampled data automatic generation control analysis with reheat steam turbines and governor dead-band effects', *IEEE Trans. Power Appar. Syst.*, 1984, **103**, (5), pp. 1045–1051
[9] Tripathy S.C., Juengst K.P.: 'Sampled data automatic generation control with superconducting magnetic energy storage in power systems', *IEEE Trans. Energy Convers.*, 1997, **12**, (2), pp. 187–192
[10] Ibraheem N., Bhatti T.S.: 'AGC of two area power system interconnected by AC/DC links with diverse sources in each area', *Int. J. Electr. Power Energy Syst., Elsevier*, 2014, **55**, pp. 297–304
[11] Shiva C.K., Mukherjee V.: 'Automatic generation control of multi-unit multi-area deregulated power system using a novel quasi-oppositional harmony search algorithm', *IET Gener. Transm. Distrib.*, 2015, **9**, (15), pp. 2398–2408
[12] Sahu R.K., Panda S., Rout U.K., *ET AL.*: 'Teaching learning based optimization algorithm for automatic generation control of power system using 2-DOF PID controller', *Int. J. Electr. Power Energy Syst., Elsevier*, 2016, **77**, pp. 287–301
[13] Shiva C.K., Mukherjee V.: 'Design and analysis of multi-source multi-area deregulated power system for automatic generation control using quasi-oppositional harmony search algorithm', *Int. J. Electr. Power Energy Syst., Elsevier*, 2016, **80**, pp. 382–395
[14] Mohanty B., Hota P.K.: 'Comparative performance analysis of fruit fly optimisation algorithm for multi-area multisource automatic generation control under deregulated environment', *IET Gener. Transm. Distrib.*, 2015, **9**, (14), pp. 1845–1855
[15] Bevrani H., Daneshfar F., Hiyama T.: 'A new intelligent agent-based AGC design with real-time application', *IEEE Trans. Syst. Man Cybern.*, 2012, **42**, (6), pp. 994–1002
[16] Chang-Chien L.R., Wu Y.S., Cheng J.S.: 'Online estimation of system parameters for artificial intelligence applications to load frequency control', *IET Gener. Transm. Distrib.*, 2011, **5**, (8), pp. 895–902
[17] Ramakrishna K.S.S., Pawan S., Bhatti T.S.: 'Automatic generation control of interconnected power system with diverse sources of power generation', *Int. J. Eng. Sci. Technol.*, 2010, **2**, (5), pp. 51–65
[18] Nikhil P., Ashu V., Bhatti T.S.: 'Study the effect of system parameters on controller gains for discrete AGC of hydro-thermal system'. IEEE Int. Conf. INDICON, 2015, pp. 1–5
[19] Sharma Y., Saikia L.C.: 'Automatic generation control of a multi-area ST – thermal power system using Grey Wolf optimizer algorithm based classical controllers', *Int. J. Electr. Power Energy Syst.*, 2015, **73**, pp. 853–862
[20] Puja D., Saikia L.C., Nidul S.: 'Automatic generation control of multi area thermal system using Bat algorithm optimized PD–PID cascade controller', *Int. J. Electr. Power Energy Syst.*, 2015, **68**, pp. 364–372
[21] Sahu R.K., Panda S., Padhan S.: 'A hybrid firefly algorithm and pattern search technique for automatic generation control of multi area power systems', *Int. J. Electr. Power Energy Syst.*, 2014, **64**, pp. 9–23
[22] Jonshagen K., Genrup M.: 'Improved load control for a steam cycle combined heat and power plant', *Energy, Elsevier*, 2010, **35**, (4), pp. 1694–1700
[23] Haisheng Y., Shuping C., Ruitao W.: 'Analysis of the sliding pressure operation for throttle controlled steam turbine generation unit'. IEEE Conf. on Power and Energy Engineering (APPEEC), Asia-Pacific, 2012, pp. 1–4
[24] Sairam A., Kaushik S.C.: 'Energy and exergy analysis of super critical thermal power plant at various load conditions under constant and pure sliding pressure', *Appl. Therm. Eng., Elsevier*, 2014, **73**, (1), pp. 51–55
[25] Eggenberger Markus A., Callan Patrick C.: 'Turbine control system for sliding or constant pressure boilers', U.S. Patent 4253308 A, 1981
[26] IEEE Committee Report: 'Dynamic models for steam and hydro turbines in power system studies', *IEEE Trans. Power Appar. Syst.*, 1973, **92**, (6), pp. 1904–1915
[27] Online resource: 'Heat balance diagram of typical coal-fired thermal power station'. Available at http://www.indianpowersector.com/home/power-station/thermal-power-plant/
[28] Ameri M., Pouria A., Armita H.: 'Energy, exergy and exergoeconomic analysis of a steam power plant: a case study', *Int. J. Energy Res.*, 2009, **33**, pp. 499–512
[29] Ion B.: 'Synchronous generators' (CRC Press, Taylor & Francis, New York, 2016, 2nd edn.), pp. 75–77
[30] Kundur P.: 'Power system stability and control' (McGraw-Hill, New York, 2009), pp. 422–424
[31] Van W.G.J., Sonntag R.E., Borgnakke C.: 'Fundamentals of thermodynamics' (John Wiley & Sons, Hoboken, NJ, USA, 2009, 7th edn.) pp. 838–877
[32] Grainger John J., Stevenson W.D.: 'Power system analysis' (McGraw-Hill, New York, 1994), pp. 703–706

## 9 Appendices

### *9.1 Appendix 1*

Coefficients of pressure–density curves

(a) For steam chest

$$C_{SC1} = -0.030063,\ C_{SC2} = -0.0026774,$$
$$C_{SC3} = 1.5478 \times 10^{-8} \text{ and } C_{SC4} = 2.464 \times 10^{-13},$$

(b) For reheater

$$C_{RH1} = -0.49492,\ C_{RH2} = 0.003372,$$
$$C_{RH3} = -6.6696 \times 10^{-8} \text{ and } C_{RH4} = 8.7542 \times 10^{-12}$$

(c) For cross-over

$$C_{CO1} = 0.00076084,\ C_{CO2} = 0.0037128,$$
$$C_{CO3} = 8.8771 \times 10^{-8} \text{ and } C_{CO4} = 1.8648 \times 10^{-12},$$


This is an open access article published by the IET under the Creative Commons Attribution License (http://creativecommons.org/licenses/by/3.0/)

Units of coefficients are

$$C_{SC1},\ C_{RH1} \text{ and } C_{Co1} = \frac{s^2}{m^2},$$

$$C_{SC2},\ C_{RH2} \text{ and } C_{CO2} = \frac{s^4}{m\,kg},$$

$$C_{SC3},\ C_{RH2} \text{ and } C_{CO3} = \frac{s^6}{kg^2},$$

$$C_{SC4},\ C_{RH4} \text{ and } C_{CO4} = \frac{s^8\,m}{kg^3},$$

### 9.2 *Appendix 2*

see Tables 9 and 10.

### 9.3 *Appendix 3*

- Case-1: At 100% loading (500 MW load)

(a) HP turbine

$$P_{HP} = \sum^{Q} (h_{in} - h_{out})$$

$$P_{HP} = Q_1(h_1 - h_2) \times 0.278\frac{kg}{s} \times 4.186\frac{kJ}{kg}$$

$$P_{HP} = [1457.009(810.7 - 728.8)]0.278\frac{kg}{s} \times 4.186\frac{kJ}{kg}$$

$$P_{HP} = 138753.24\frac{kJ}{s} \quad \text{or} \quad kW = 138.864\,MW$$

(b) IP turbine

$$P_{IP} = \sum^{Q} (h_{in} - h_{out})$$

$$P_{IP} = [Q_{22}(h_{22} - h_6) + (Q_{22} - Q_6)(h_6 - h_8)] \times 0.278\frac{kg}{s} \times 4.186\frac{kJ}{kg}$$

$$P_{IP} = [1301.229(858.2 - 800.1)\ (1301.229 - 87.418) \times (800.1 - 735.8)]0.278\frac{kg}{s} \times 4.186\frac{kJ}{kg}$$

$$P_{IP} = 178.837\,MW$$

(c) LP turbine

$$P_{LP} = \sum^{Q} (h_{in} - h_{out})$$

$$P_{LP} = [Q_{21}(h_{21} - h_{10}) + (Q_{21} - Q_{10})(h_{10} - h_{12}) + (Q_{21} - Q_{10} - Q_{12})(h_{12} - h_{14}) + Q_{20}(h_{14} - h_{20})] \times 0.278\frac{kg}{s} \times 4.186\frac{kJ}{kg}P_{LP} = [1086.754(735.8 - 689)\ (1086.754 - 40.720) \times (689 - 661.3)\ (1086.754 - 40.720 - 71.96) \times$$

**Table 9** Heat balance data of 500 MW power generation unit at different loads

| Location | Pressure, kgf/cm$^2$ | | | | | | Enthalpy, kcal/kg | | | |
|---|---|---|---|---|---|---|---|---|---|---|
| | 100% Loading | 80% Loading | 60% Loading | 50% Loading | 30% Loading | 100% Loading | 80% Loading | 60% Loading | 50% Loading | 30% Loading |
| 1 | 170.0 | 170.0 | 170.0 | 170.0 | 170.0 | 810.7 | 810.7 | 810.7 | 810.7 | 783.2 |
| 2 | 45.00 | 36.42 | 28.06 | 22.87 | 14.37 | 728.8 | 729.2 | 729.8 | 726.39 | 703.925 |
| 3 | 45.00 | 36.42 | 28.06 | 22.87 | 14.37 | 728.8 | 729.2 | 729.8 | 726.39 | 703.925 |
| 4 | 42.75 | 34.92 | 27.14 | 22.20 | 14.00 | 728.8 | 729.2 | 729.8 | 726.39 | 703.925 |
| 5 | – | – | – | – | – | 126.9 | 201.8 | 191.4 | 183.6 | 163.7 |
| 6 | 18.32 | 14.90 | 11.52 | 9.520 | 6.050 | 800.1 | 801.6 | 803.2 | 804.3 | 763.1 |
| 7 | 17.40 | 14.20 | 11.04 | 9.160 | 5.990 | 800.1 | 801.6 | 803.2 | 804.3 | 763.1 |
| 8 | 7.130 | 5.810 | 4.490 | 3.910 | 2.740 | 735.8 | 737.2 | 738.6 | 730.915 | 697.46 |
| 9 | 6.560 | 5.410 | 4.230 | 3.710 | 3.650 | 735.6 | 737.2 | 738.6 | 730.915 | 686.43 |
| 10 | 2.828 | 2.314 | 1.794 | 1.565 | 1.004 | 689.0 | 690.3 | 691.6 | 694.3 | 668.8 |
| 11 | – | – | – | – | – | 106.5 | 101.1 | 94.90 | 91.70 | 81.90 |
| 12 | 1.487 | 1.198 | 0.935 | 0.819 | 0.544 | 661.3 | 661.9 | 663.2 | 665.6 | 644.5 |
| 13 | – | – | – | – | – | 68.40 | 65.50 | 61.00 | 58.40 | 50.80 |
| 14 | 0.351 | 0.292 | 0.226 | 0.196 | 0.132 | 608.6 | 609.9 | 610.7 | 611.8 | 612.6 |
| 15 | 0.333 | 0.282 | 0.222 | 0.194 | 0.132 | 608.6 | 609.9 | 610.7 | 611.8 | 612.6 |
| 16 | – | – | – | – | – | 49.70 | 49.30 | 48.80 | 48.60 | 48.10 |
| 17 | – | – | – | – | – | 47.20 | 47.30 | 47.50 | 47.60 | 47.90 |
| 18 | 22.000 | 24.390 | 26.19 | 26.82 | 27.63 | 47.00 | 47.10 | 47.20 | 47.30 | 47.50 |
| 19 | 0.1047 | 0.1047 | 0.1047 | 0.1047 | 0.1047 | 46.30 | 46.30 | 46.30 | 46.30 | 46.30 |
| 20 | 0.1047 | 0.1047 | 0.1047 | 0.1047 | 0.1047 | 573.2 | 579.5 | 590.4 | 599.2 | 603.9 |
| 21 | 7.1300 | 5.8100 | 4.4900 | 3.9100 | 2.7400 | 735.8 | 737.2 | 738.6 | 730.837 | 682.110 |
| 22 | 40.500 | 32.810 | 25.260 | 20.610 | 12.980 | 858.2 | 859.8 | 861.4 | 862.4 | 815.8 |
| 23 | – | – | – | – | – | 99.80 | 99.80 | 99.80 | 99.80 | 99.90 |
| 24 | – | – | – | – | – | 51.80 | 50.60 | 49.40 | 48.90 | 48.20 |
| 25 | – | – | – | – | – | 71.10 | 67.30 | 61.90 | 58.90 | 50.90 |
| 26 | – | – | – | – | – | 73.10 | 69.10 | 63.70 | 60.70 | 52.00 |
| 27 | – | – | – | – | – | 111.2 | 105.1 | 98.10 | 94.40 | 83.70 |
| 28 | – | – | – | – | – | 107.8 | 161.7 | 151.2 | 145.7 | 145.0 |
| 29 | – | – | – | – | – | 214.2 | 204.0 | 192.1 | 183.5 | 162.5 |
| 30 | – | – | – | – | – | 263.4 | 251.4 | 237.2 | 225.9 | 201.0 |

This is an open access article published by the IET under the Creative Commons Attribution License (http://creativecommons.org/licenses/by/3.0/)

**Table** 10 Heat balance data of 500 MW power generation unit at different loads

| Location | Flow, t/h | | | | | Temperature, °C | | | | |
|---|---|---|---|---|---|---|---|---|---|---|
| | 100% Loading | 80% Loading | 60% Loading | 50% Loading | 30% Loading | 100% Loading | 80% Loading | 60% Loading | 50% Loading | 30% Loading |
| 1 | 1457.009 | 1166.642 | 887.632 | 755.373 | 552.646 | 537.0 | 537.0 | 537.0 | 537.0 | 497.0 |
| 2 | 1301.229 | 1051.563 | 808.262 | 656.828 | 437.216 | 337.0 | 329.2 | 321.5 | 310.7 | 255.9 |
| 3 | 149.644 | 110.122 | 75.558 | 95.434 | 113.636 | 337.0 | 329.2 | 321.5 | 310.7 | 255.9 |
| 4 | 149.644 | 110.122 | 75.558 | 58.824 | 38.129 | 334.8 | 327.6 | 320.5 | 310.0 | 255.3 |
| 5 | 1457.009 | 1166.642 | 887.632 | 755.373 | 552.646 | 204.8 | 196.6 | 186.7 | 179.2 | 159.9 |
| 6 | 87.418 | 68.478 | 50.422 | 39.413 | 13.767 | 445.0 | 446.0 | 447.1 | 448.0 | 363.7 |
| 7 | 87.418 | 68.478 | 50.422 | 39.413 | 13.767 | 444.5 | 445.5 | 446.8 | 447.8 | 363.6 |
| 8 | 130.184 | 102.042 | 78.980 | 29.646 | 00.00 | 309.9 | 311.4 | 312.8 | 319.5 | 261.2 |
| 9 | 66.966 | 50.879 | 36.028 | 29.646 | 33.478 | 309.3 | 311.0 | 312.5 | 319.3 | 237.9 |
| 10 | 40.720 | 31.823 | 22.994 | 19.111 | 12.690 | 280.7 | 210.3 | 211.9 | 217.1 | 161.9 |
| 11 | 1152.981 | 937.163 | 725.624 | 627.49 | 467.272 | 106.2 | 100.9 | 94.8 | 91.6 | 81.8 |
| 12 | 71.960 | 54.349 | 39.771 | 33.474 | 23.830 | 148.0 | 148.1 | 150.0 | 154.4 | 108.2 |
| 13 | 1152.981 | 937.163 | 725.624 | 627.490 | 467.272 | 68.3 | 65.4 | 60.9 | 58.3 | 50.7 |
| 14 | 39.658 | 27.626 | 15.849 | 10.905 | 2.261 | 0.9644 | 0.9701 | 0.9759 | 0.9801 | 0.9572 |
| 15 | 39.658 | 27.626 | 15.849 | 10.905 | 2.261 | 0.9644 | 0.9701 | 0.9759 | 0.9801 | 0.9572 |
| 16 | 1152.981 | 937.163 | 725.624 | 627.49 | 467.272 | 49.6 | 49.2 | 48.7 | 48.5 | 48.0 |
| 17 | 1152.981 | 937.163 | 725.624 | 627.49 | 467.272 | 47.0 | 47.2 | 47.4 | 47.5 | 47.6 |
| 18 | 1152.981 | 937.163 | 725.624 | 627.49 | 467.272 | 46.6 | 46.6 | 46.7 | 46.7 | 47.0 |
| 19 | 1152.981 | 937.163 | 726.624 | 627.49 | 467.272 | 46.4 | 46.4 | 46.4 | 46.4 | 46.4 |
| 20 | 934.862 | 770.214 | 602.647 | 526.237 | 386.371 | 0.9223 | 0.9335 | 0.9524 | 0.9679 | 0.976 |
| 21 | 1086.754 | 883.566 | 680.817 | 589.281 | 424.432 | 309.9 | 311.4 | 312.8 | 319.5 | 261.2 |
| 22 | 1301.229 | 1051.563 | 808.262 | 656.828 | 437.216 | 565.0 | 565.0 | 565.0 | 565.0 | 472.0 |
| 23 | 0.356 | 0.355 | 0.355 | 0.353 | 0.283 | 99.7 | 99.7 | 99.7 | 99.7 | 99.9 |
| 24 | 152.338 | 113.798 | 78.614 | 63.490 | 38.781 | 51.8 | 50.6 | 49.4 | 48.9 | 48.2 |
| 25 | 152.338 | 113.798 | 78.614 | 63.490 | 38.781 | 71.1 | 67.3 | 61.9 | 59.0 | 50.9 |
| 26 | 112.68 | 86.172 | 62.765 | 52.585 | 36.520 | 73.1 | 69.1 | 63.7 | 60.7 | 52.0 |
| 27 | 40.720 | 31.823 | 22.994 | 19.111 | 12.690 | 111.0 | 105.0 | 98.0 | 94.4 | 83.6 |
| 28 | 237.062 | 178.60 | 125.980 | 98.237 | 51.896 | 169.0 | 160.2 | 150.1 | 144.8 | 144.2 |
| 29 | 149.644 | 110.122 | 75.558 | 58.824 | 38.129 | 209.6 | 200.2 | 189.2 | 181.0 | 161.0 |
| 30 | 1457.009 | 1166.642 | 887.632 | 755.373 | 552.646 | 253.4 | 242.7 | 229.8 | 219.4 | 195.9 |

$$(661.3 - 608.6)\ (934.862)(608.6 - 573.2)]\ 0.278\frac{\text{kg}}{\text{s}} \times 4.186\frac{\text{kJ}}{\text{kg}}$$

$$P_{\text{LP}} = 191.439\,\text{MW}$$

Total power output ($P_{\text{T}}$) = 138.864 MW + 178.837 MW + 191.439 MW = 509.173 MW.

Mechanical losses = 1.444 MW.

Generator losses = 7.579 MW.

Power required by turbine-generator (TG) auxiliary = 0.150 MW.

Net turbine output = (total power output) – (mechanical losses + generator losses + TG auxiliary supply).

$P_{\text{net}}$ = 509.173 MW – (1.444 MW + 7.579 MW + 0.150 MW).

$P_{\text{net}}$ = 500 MW.

The power fractions of HP, IP and LPTs are as follows

$$a_1 = \frac{P_{\text{LP}}}{P_{\text{HP}}} = 1.3786,\ \ a_2 = \frac{P_{\text{IP}}}{P_{\text{HP}}} = 1.2875$$

$$F_{\text{HP}} = \frac{1}{1 + a_1 + a_2} = 0.2727$$

$$F_{\text{IP}} = \frac{a_2}{1 + a_1 + a_2} = 0.3511$$

$$F_{\text{LP}} = \frac{a_1}{1 + a_1 + a_2} = 0.3760$$

- Case-2: At 80% loading (400 MW load)

(a) HP turbine

$$P_{\text{HP}} = \sum\nolimits^{Q} (h_{\text{in}} - h_{\text{out}})$$

$$P_{\text{HP}} = [1166.642(810.7 - 729.2)]0.278\frac{\text{kg}}{\text{s}} \times 4.186\frac{\text{kJ}}{\text{kg}}$$

$$P_{\text{HP}} = 110646.89\frac{\text{kJ}}{\text{s}} \quad \text{or} \quad \text{kW} = 110.646\,\text{MW}$$

(b) IP turbine

$$P_{\text{IP}} = \sum_{k=1}^{2} Q_k(h_{\text{in},k} - h_{\text{out},k})$$

$$P_{\text{IP}} = [1051.563(859.8 - 801.6)$$

$$\times (1051.563 - 68.478)(801.6 - 737.2)]0.278\frac{\text{kg}}{\text{s}} \times 4.186\frac{\text{kJ}}{\text{kg}}$$

$$P_{\text{IP}} = 144.895\,\text{MW}$$

(c) LP turbine

$$P_{\text{LP}} = \sum_{k=1}^{4} Q_k(h_{\text{in},k} - h_{\text{out},k})$$


This is an open access article published by the IET under the Creative Commons Attribution License (http://creativecommons.org/licenses/by/3.0/)

$$P_{LP} = [883.566(737.2 - 690.3)\ (883.566 - 54.349) \times (690.3 - 661.9)\ (883.566 - 54.349 - 27.626) \times (661.9 - 609.9)\ (770.214)(609.9 - 579.5)]0.278$$

$$\frac{\text{kg}}{\text{s}} \times 4.186 \frac{\text{kJ}}{\text{kg}} P_{LP} = 151.382\,\text{MW}$$

Total power output ($P_T$) = 110.646 MW + 144.895 MW + 151.382 MW = 406.923 MW.

Mechanical losses = 1.444 MW.

Generator losses = 5.329 MW.

Power required by TG auxiliary = 0.150 MW.

Net turbine output = (total power output) – (mechanical losses + generator losses + TG auxiliary supply).

$P_{net}$ = 406.923 MW – (1.444 MW + 5.329 MW + 0.150 MW).

$P_{net}$ = 400 MW

$$a_1 = \frac{P_{LP}}{P_{HP}} = 1.3681\ ,\ a_2 = \frac{P_{IP}}{P_{HP}} = 1.30956$$

$$F_{HP} = \frac{1}{1 + a_1 + a_2} = 0.2719$$

$$F_{IP} = \frac{a_2}{1 + a_1 + a_2} = 0.3560$$

$$F_{LP} = \frac{a_1}{1 + a_1 + a_2} = 0.3720$$

### 9.4 Appendix 4

Thermal–thermal power system model parameter values are calculated as follows (see Table 11).

**Table 11** Calculated parameters of two area AGC thermal power system model

| Parameters | Area-1 | Area-2 |
|---|---|---|
| area capacities | $P_{r1}$ = 2000 MW | $P_{r2}$ = 1000 MW |
| rating of single generating machine | $S$ = 500 MW | $S$ = 500 MW |
| speed droop of single unit on machine base | 2.4 Hz/MW | 2.4 Hz/MW |
| speed droop of single unit on power system area base | $R = \frac{2.4}{(500/2000)} = 9.6$ Hz/MW pu. | $R = \frac{2.4}{(500/1000)} = 4.8$ Hz/MW pu. |
| number of generating units | $n = 4$ | $n = 2$ |
| equivalent speed droop characteristic for area-1 and area-2 | $R_{eqv1} = \frac{1}{(1/R + 1/R + 1/R + 1/R)}$ $R_{eqv1} = \frac{R}{4} = \frac{9.6}{4} = 2.4$ Hz/MW pu. | $R_{eqv2} = \frac{1}{(1/R + 1/R)}$ $R_{eqv2} = \frac{R}{2} = \frac{4.8}{2} = 2.4$ Hz/MW pu. |
| inertia constant of single generating unit | $H$ = 5 s | $H$ = 5 s |
| equivalent inertia constant for area-1 and area-2 | $H_{eqv1} = \frac{H_1S_1 + H_2S_2 + H_3S_3 + H_4S_4}{S_{system}}$ | $H_{eqv1} = \frac{(5 \times 500) + (5 \times 500) + (5 \times 500) + (5 \times 500)}{2000}$ |
| $H_{eqv1}$ = 5 s | $H_{eqv2} = \frac{H_1S_1 + H_2S_2}{S_{system}}$ | $H_{eqv2} = \frac{H_1S_1 + H_2S_2}{S_{system}}$ |
| | $H_{eqv2} = \frac{(5 \times 500) + (5 \times 500)}{1000} H_{eqv2} = 5$ s | $H_{eqv2} = \frac{(5 \times 500) + (5 \times 500)}{1000} H_{eqv2} = 5$ s |
| system frequency | 60 Hz | |
| synchronising coefficient | $2\pi T_{12}$ = 0.545 pu MW | |
| maximum tie-line power transfer limit | $P_{tie\ max}$ = 200 MW | |
| maximum allowable angle difference | $\delta_1 - \delta_2 = 30°$ | |
| area capacity ratios | $a_{12} = -P_{r1}/P_{r2} = -2$ | |
| $T_{p1}$, $T_{p2}$, $K_{P1}$, $K_{P2}$, $B_1$, $B_2$ | the values are calculated at different generation schedules shown in Table 6 | |
| $F_{HPi}$, $F_{IPi}$ and $F_{LPi}$ | the values are calculated at different generation schedules shown in Table 5 | |
| $T_{CHi}$, $T_{RHi}$ and $T_{COi}$ | the values are calculated at different generation schedules shown in Tables 1–3 | |

This is an open access article published by the IET under the Creative Commons Attribution License (http://creativecommons.org/licenses/by/3.0/)



View publication stats